Electronic Supplementary Information: On the Stabilization of Ferroelectric Negative Capacitance in Nanoscale Devices

Michael Hoffmann,*,† Milan Pešić,† Stefan Slesazeck,† Uwe Schroeder,† and Thomas Mikolajick†,‡

†*NaMLab gGmbH, Noethnitzer Str. 64, D-01187, Dresden, Germany*

‡*Chair of Nanoelectronic Materials, TU Dresden, D-01062 Dresden, Germany*

E-mail: michael.hoffmann@namlab.com

S1. Derivation of Eq. 2 and MFMIM Landau Free Energy Simulations

Here, a detailed derivation of Eq. 2 will be given. To obtain the Helmholtz free energy per volume for an alternating domain pattern as shown in Fig. 1(b), we first consider the ferroelectric anisotropy energy of the domains. Since one half of the film has domains with polarization P_1 and the other half with P_2 we can write:

$$u_{anisotropy} = \frac{1}{2}\left(\alpha P_1^2 + \beta P_1^4\right) + \frac{1}{2}\left(\alpha P_2^2 + \beta P_2^4\right) = \frac{\alpha}{2}(P_1^2 + P_2^2) + \frac{\beta}{2}(P_1^4 + P_2^4). \tag{S1}$$

To obtain the domain wall energy contribution u_{DW} of the whole film one has to find expressions for the energy density of a single domain wall $U_{single,DW}$ per area, the number

of domain walls in the sample N_{DW}, multiply both terms and normalize them to the lateral film length L, i.e.

$$u_{DW} = \frac{U_{single,DW} N_{DW}}{L}. \tag{S2}$$

The energy density of a single domain wall is given by

$$U_{single,DW} = wk\left(\nabla P\right)^2 = wk\frac{(P_1 - P_2)^2}{w^2} = k\frac{(P_1 - P_2)^2}{w}. \tag{S3}$$

Since $L = nd$, where $n = 1, 2, 3, ...$, we can write down the total number of domain walls as

$$N_{DW} = \frac{2L}{d} - 1. \tag{S4}$$

Now we can combine all of these expressions to obtain the domain wall energy contribution per sample volume as

$$u_{DW} = \frac{U_{single,DW} N_{DW}}{L} = \frac{1}{L}\left(\frac{2L}{d} - 1\right)\frac{k}{w}(P_1 - P_2)^2 = \left(\frac{2}{d} - \frac{1}{L}\right)\frac{k}{w}(P_1 - P_2)^2. \tag{S5}$$

The total ferroelectric free energy density per volume in Eq. 2 is then obtained as

$$u_F = u_{anisotropy} + u_{DW} + \frac{\varepsilon_0 \varepsilon_b}{2} E_F^2, \tag{S6}$$

where the last term is due to the electrostatic self-energy, which is the same as in the homogeneous case.

For the multi-domain ferroelectric energy landscape shown in Fig. 2, the simulation parameters $\alpha = -4 \times 10^7$ m/F and $\beta = 4.2 \times 10^7$ m^5/(C^{2}F) were used. For the MFMIM simulations shown in Fig. 3, the same ferroelectric anisotropy constants were applied. Additionally, we defined $\varepsilon_b = 100$, $t_D = 10$ nm, $\varepsilon_r = 1312$ and $k/(wL_{crit}) = 10^7$ m^{-1}F^{-1}. All

MFMIM simulations are based on Eq. 2 and 3 in the main text.

S2. MFIM 2D Electrostatics Simulations

To solve the electrostatics of a metal/ferroelectric/insulator/metal (MFIM) structure in the absence of magnetic fields, we start from Faraday's law of induction which yields

$$\nabla \times E = 0. \tag{S7}$$

Eq. S7 is always valid for a scalar electrostatic potential φ, which is related to the electric field E by

$$E = -\nabla\varphi. \tag{S8}$$

Next we use Gauss's law which is given by

$$\nabla \cdot D = \rho_{free}, \tag{S9}$$

where D is the electric displacement field and ρ_{free} is the density of free charges per volume. Assuming we have an anisotropic linear dielectric with relative permittivies ε_x and ε_z in the in-plane and out-of-plane directions, respectively (see Fig. 1), with spontaneous the polarization P_z only in z-direction we can write

$$D = \varepsilon_0 \begin{pmatrix} \varepsilon_x & 0 \\ 0 & \varepsilon_z \end{pmatrix} E + \begin{pmatrix} 0 \\ P_z \end{pmatrix} = \begin{pmatrix} -\varepsilon_0 \varepsilon_x \frac{\partial \varphi}{\partial x} \\ -\varepsilon_0 \varepsilon_z \frac{\partial \varphi}{\partial z} + P_z \end{pmatrix}, \tag{S10}$$

to relate φ and P_z to D. If we now assume that we have no free charges in the structure ($\rho_{free} = 0$) and consider that ε_x and ε_z are functions of position, we can insert Eq. S10 into Eq. S9 and obtain

$$\nabla \cdot D = \frac{\partial \varepsilon_x}{\partial x}\frac{\partial \varphi}{\partial x} + \frac{\partial \varepsilon_z}{\partial z}\frac{\partial \varphi}{\partial z} + \varepsilon_x \frac{\partial^2 \varphi}{\partial x^2} + \varepsilon_z \frac{\partial^2 \varphi}{\partial z^2} - \frac{1}{\varepsilon_0}\frac{\partial P_z}{\partial z} = 0. \tag{S11}$$

Eq. S11 can now be solved for φ if $P_z(z,x)$, $\varepsilon_x(z,x)$ and $\varepsilon_z(z,x)$ as well as appropriate electrostatic boundary conditions are given. To numerically solve Eq. S11 we apply a simple finite difference approach, which is used to approximate the derivatives of a function $f(x)$ as

$$\begin{aligned} \frac{\partial f}{\partial x} &\approx \frac{f_{x+1} - f_x}{\Delta x}, \\ \frac{\partial^2 f}{\partial x^2} &\approx \frac{f_{x+1} - 2f_x + f_{x-1}}{\Delta x^2}, \end{aligned} \tag{S12}$$

where f_{x+1} and f_{x-1} are discretized values of f adjacent to the grid value f_x, where the derivative is taken and Δx is the numerical grid spacing in x-direction. Analogously to Eq. S12, the derivatives in z-direction are obtained by substituting x with z. Using this method to discretize Eq. S11 we can write down a formula for the electrostatic potential φ at the grid point (z,x) as

$$\varphi_{zx} = \frac{\left(\varepsilon_x \varphi_{x-1} + \varepsilon_{x+1}\varphi_{x+1}\right)\Delta z^2 + \left(\varepsilon_z \varphi_{z-1} + \varepsilon_{z+1}\varphi_{z+1}\right)\Delta x^2 + \left(P_z - P_{z+1}\right)\Delta z \Delta x^2/\varepsilon_0}{\left(\varepsilon_x + \varepsilon_{x+1}\right)\Delta z^2 + \left(\varepsilon_z + \varepsilon_{z+1}\right)\Delta x^2}, \tag{S13}$$

where Δz is the grid spacing in z-direction. Indices in Eq. S13 indicate the grid position relative to (z,x). In addition to Eq. S13 we also need electrostatic boundary conditions to calculate φ. If we define a numerical grid of dimensions $Z \times X$, where $z = 1, 2, ..., Z$ and $x = 1, 2, ..., X$, we can then define $z = 1$ as the top and $z = Z$ as the bottom electrode of the capacitor structure. For the short-circuit condition of both electrodes we then obtain

$$\varphi(z = 1, x) = \varphi(z = Z, x) = 0. \tag{S14}$$

Furthermore, to be able to simulate an infinite capacitor structure in x-direction we apply

periodic boundary conditions at the remaining edges of the grid as

$$\begin{aligned}\varphi(z, x = 0) &= \varphi(z, x = X),\\ \varphi(z, x = 1) &= \varphi(z, x = X + 1).\end{aligned} \tag{S15}$$

To solve Eq. S13, an iterative algorithm was used where the electrostatic potential of the current iteration $\varphi^{(i)}$ is calculated from the value of the last iteration $\varphi^{(i-1)}$. At each iteration step (i), the remaining error at each grid point is calculated as

$$\epsilon^{(i)} = \left| \frac{\varphi^{(i-1)} - \varphi^{(i)}}{\varphi^{(i-1)}} \right|. \tag{S16}$$

This process is repeated until the maximum error for φ is below 0.01 % or

$$\max(\epsilon^{(i)}) < 10^{-4}. \tag{S17}$$

From φ, E and D are then easily obtained from Eq. S8 and Eq. S10, respectively. The free energy density per unit volume at each grid point (z, x) is then calculated as

$$u(z, x) = \alpha P^2 + \beta P^4 + k \left(\frac{P(z, x) - P(z, x + 1)}{\Delta x} \right)^2 + \frac{1}{2} ED, \tag{S18}$$

where P is only the spontaneous polarization, which is zero in the dielectric region. To calculate the total free energy of an infinite capacitor in x- and y-direction per unit area we can use the equation

$$U_T = \frac{1}{d} \sum_{x=1}^{X} \sum_{z=1}^{Z} u(z, x) \Delta x \Delta z, \tag{S19}$$

where $d = X\Delta x$ is the domain period as defined in Fig. 1(b). The simulation parameters used for the results shown in Fig. 4 for the ferroelectric were $\alpha = -4 \times 10^7$ m/F, $\beta = 4.2 \times 10^7$ $\mathrm{m^5/(C^2F)}$, $k/w = 4.65 \times 10^{-2}$ $\mathrm{m^2F^{-1}}$, $X = 100$, $\Delta x = d/X$, $\Delta z = 5 \times 10^{-11}$ m and

$\varepsilon_x = \varepsilon_z = \varepsilon_b = 30$. For the dielectric, $\varepsilon_x = \varepsilon_z = \varepsilon_r = 400$ was used. It should be noted that Z was changed depending on the total thickness $t_D + t_F$ to keep Δz constant for all simulations. This ensured a clearly defined grid position of the ferroelectric/dielectric interface. Furthermore, for all simulations we have checked that Δx and Δz are sufficiently small such that no change of the result was observed when reducing them further.

S3. MFIM: Domain Formation as a Function of t_D

Figure S1 shows the region of NC stabilization in the MFIM structure as a function of the dielectric thickness t_D. The critical ferroelectric thickness for domain formation $t_{F,dw}$ is shown normalized to the value of $t_{F,dw}$ for $t_D >> d_{eq}$, where d_{eq} is the equilibrium domain period when t_D is large. Fig. S1 shows, that if t_D is smaller than $d_{eq}/2$, the critical maximum thickness for NC stability rapidly drops to zero. The reason for this is the interaction of the polarization charges with the bottom electrode, which favors domain formation over the NC state.

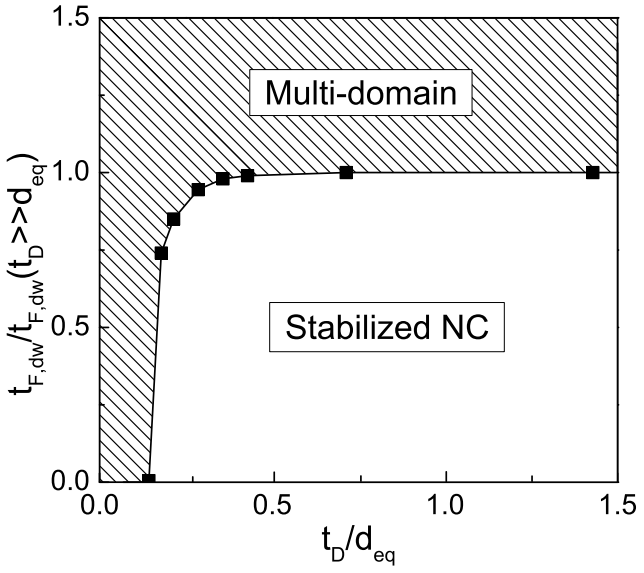

Figure S1: Region of NC stabilization in an MFIM structure as a function of t_D. The critical thickness for domain formation is normalized to the value for the limit where $t_D >> d_{eq}$. t_D is normalized to the equilibrium domain period d_{eq} in the same limit.

S5. Estimations for Different Ferroelectric Materials

In Table S1 we have compiled material parameters for typical ferroelectrics and calculated L_{crit}. The parameters for $BaTiO_3$ were taken from W. Kinase and H. Takahasi [Journal of the Physical Society of Japan 12, 464-476 (1957)], Y. Cao et al. [Appl. Phys. Lett. 104, 182905 (2014)] and X. Lu et al. [J. Appl. Phys. 114, 224106 (2013)]. Values for $PbTiO_3$ were taken from R.K. Behera et al. [J. Phys.: Condens. Matter 23, 175902 (2011)], A.N. Morozovska et al. [Phys. Rev. B 80, 214110 (2009)] and M.J. Haun et al. [J. Appl. Phys. 62, 3331-3338 (1987)]. The domain wall coupling constants k were obtained from the formula $k = \sigma_{DW} w/(4P_S^2)$ where P_S is the spontaneous polarization of the anti-parallel domains in the ferroelectric and σ_{DW} is the domain wall energy density per area. Values for ferroelectric HfO_2 were estimated based on S. Clima et al. [Appl. Phys. Lett. 104, 092906 (2014)]. Domain wall energy constants for HfO_2 have not been reported so far. From Table S1 it can be seen that L_{crit} is in the order of 1 nm for perovskite ferroelectrics, which makes the use of an MFMIM structure impractical for NC devices as discussed in the main text. The domain coupling term $k/w = 4.65 \times 10^{-2}$ m^2/F, which we used for simulation of the MFIM structure, is slightly smaller compared e.g. to $PbTiO_3$ with $k/w = 5.83 \times 10^{-2}$ m^2/F, but larger than $BaTiO_3$ with $k/w = 7.13 \times 10^{-3}$ m^2/F.

Table S1: Material parameters for typical ferroelectrics from literature and calculated critical lateral dimension L_{crit}.

Parameter	**$BaTiO_3$**	**$PbTiO_3$**	**HfO_2**	**Units**
$\alpha(T = 300\ \text{K})$	-2.89×10^7	-1.72×10^8	-1×10^9	m/F
ε_b	45	67	25	1
k	2.85×10^{-12}	4.55×10^{-11}	?	m^3/F
w	4×10^{-10}	7.81×10^{-10}	5×10^{-10}	m
P_S	0.2216	0.867	0.5	C/m^2
DW energy density	0.0014	0.175	?	J/m^2
L_{crit}	9.86×10^{-10}	1.36×10^{-9}	?	m

Calculations for the critical ferroelectric dimensions $t_{F,dw}$, $t_{F,max}$ and L_{crit} as a function of the relative dielectric permittivity ε_r and t_D for $PbTiO_3$ and $BaTiO_3$ are shown in Fig. S2

and Fig. S3, respectively. The ferroelectric material parameters were taken from Table S1 at 300 K. It can be seen that in all cases, $t_{F,dw}$ is significantly smaller compared to $t_{F,max}$, which again shows why it is critical to consider domain formation when assessing the stabilization of NC in ferroelectrics.

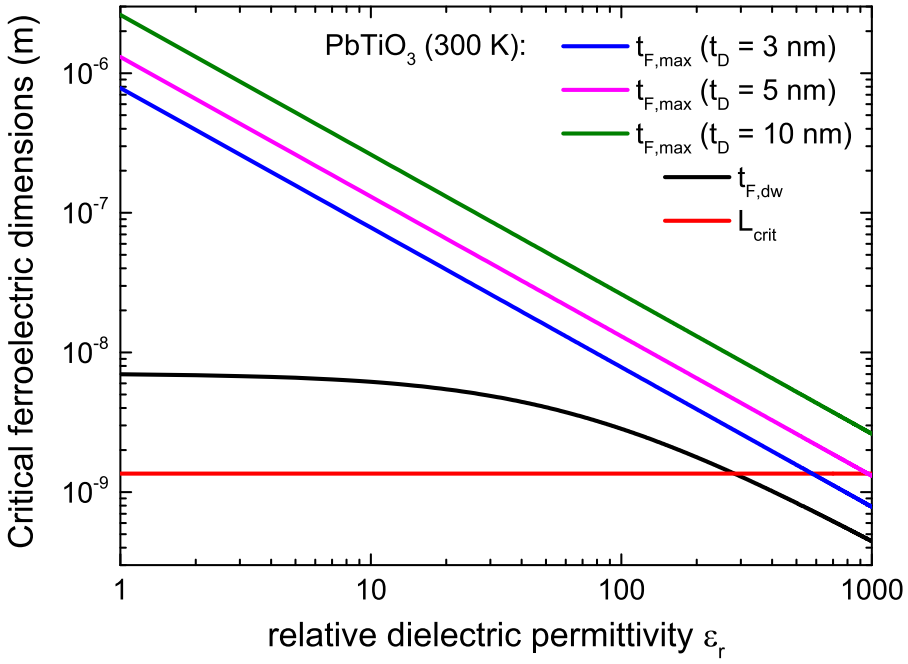

Figure S2: Critical ferroelectric dimensions $t_{F,dw}$, $t_{F,max}$ and L_{crit} in a MFIM capacitor as a function of ε_r for different dielectric thicknesses t_D for $PbTiO_3$ material parameters taken from Table S1.

While L_{crit} is completely independent of ε_r, both $t_{F,dw}$ and $t_{F,max}$ significantly drop with increasing ε_r. Furthermore, $t_{F,max}$ scales linearly with t_D, since it is inversely proportional to C_D. Comparing $PbTiO_3$ and $BaTiO_3$ it can be seen that the latter has a significantly larger $t_{F,dw}$ due to the larger value of α at 300 K. It should be noted that all these considerations are based on the assumptions of an infinite film, closed electric field lines in the dielectric (see section S3) and no in-plane spontaneous polarization contributions in the ferroelectric.

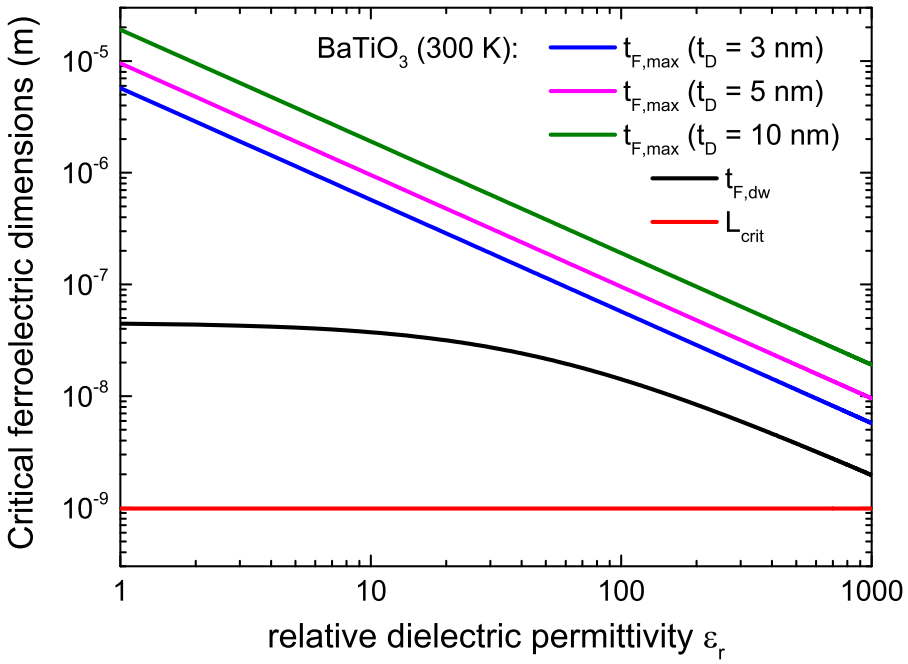

Figure S3: Critical ferroelectric dimensions $t_{F,dw}$, $t_{F,max}$ and L_{crit} in a MFIM capacitor as a function of ε_r for different dielectric thicknesses t_D for $BaTiO_3$ material parameters taken from Table S1.